Chemical properties of lipids strongly affect the kinetics of the membrane-induced aggregation of α-synuclein

Céline Galvagnion[a], James W. P. Brown[a], Myriam M. Ouberai[b], Patrick Flagmeier[a], Michele Vendruscolo[a], Alexander K. Buell[a,1], Emma Sparr[c], and Christopher M. Dobson[a,2]

[a]Department of Chemistry, University of Cambridge, Cambridge CB2 1EW, United Kingdom; [b]Nanoscience Centre, Department of Engineering, University of Cambridge, Cambridge CB3 0FF, United Kingdom; and [c]Division of Physical Chemistry, Chemistry Department, Lund University, 22100 Lund, Sweden

Edited by Michael L. Klein, Temple University, Philadelphia, PA, and approved May 9, 2016 (received for review February 10, 2016)

Intracellular α-synuclein deposits, known as Lewy bodies, have been linked to a range of neurodegenerative disorders, including Parkinson's disease. α-Synuclein binds to synthetic and biological lipids, and this interaction has been shown to play a crucial role for both α-synuclein's native function, including synaptic plasticity, and the initiation of its aggregation. Here, we describe the interplay between the lipid properties and the lipid binding and aggregation propensity of α-synuclein. In particular, we have observed that the binding of α-synuclein to model membranes is much stronger when the latter is in the fluid rather than the gel phase, and that this binding induces a segregation of the lipids into protein-poor and protein-rich populations. In addition, α-synuclein was found to aggregate at detectable rates only when interacting with membranes composed of the most soluble lipids investigated here. Overall, our results show that the chemical properties of lipids determine whether or not the lipids can trigger the aggregation of α-synuclein, thus affecting the balance between functional and aberrant behavior of the protein.

α-synuclein | Parkinson's disease | phase diagram | lipid-induced aggregation

The protein α-synuclein is mainly found in the presynaptic termini of neurons (1). The protein has been shown to populate a highly unstructured form in its unbound state both in vitro and in vivo and to adopt an α-helical conformation when bound to membranes (2). The balance between these two states has been found to play a role both in the proposed biological function of the protein, including the regulation of synaptic plasticity, and in the kinetics of its pathogenic aggregation; the latter is the hallmark of a range of diseases, known as synucleinopathies, of which the most common is Parkinson's disease (3, 4). α-Synuclein has been shown to have its highest affinity for membranes containing either anionic lipids or so-called "packing defects" (5–7), where the latter are defined as low-density regions in bilayers with high exposure of the lipid hydrophobic chains attributable to a mismatch between lipid shape and bilayer curvature (6, 7).

Biological membranes are highly heterogeneous and differ from one cell or organelle to another in terms of the physical and chemical properties of the membranes, including curvature, charge, fluidity, and packing of the hydrophobic chains (8–10). The variety of membrane structures in cells can be directly related to differences in lipid (and protein) composition, where properties such as length and saturation of the hydrocarbon chain as well as the charge and size of the polar head group are crucial in determining the properties of the membrane (8, 9). In particular, most chemical and thermotropic properties of a lipid molecule are known to vary almost linearly with the length of its hydrophobic chain. As some examples, the standard change in free energy of transfer of a lipid molecule from water into a bilayer (i.e., its solubility in water), the melting temperature, and the enthalpy of melting have all been found to be proportional to the number of aliphatic carbons in the hydrophobic chain, which ranges from 8 to 18 (11). In addition, the adsorption and partitioning of small molecules and proteins to membranes can also affect the structural and thermotropic properties of the latter, and the magnitude and characteristics of these changes depend on the nature of the molecular interactions (e.g., electrostatic, hydrophobic) (12, 13).

The interactions between amphipathic proteins and membranes have been extensively studied over the last three decades (7, 14–22). In general, the amino acid sequences of these peripheral proteins are characterized by patterns of hydrophobic and polar residues such that the proteins fold into amphipathic α-helices upon binding to hydrophobic patches exposed at the membrane interface (16, 17). In particular, molecular dynamics simulations and neutron reflectometry studies of deposited bilayers have shown that the amphipathic helix in α-synuclein is primarily located in the vicinity of the lipid phosphate groups and the glycerol backbone (16, 23–25).

Although the binding of α-synuclein to membranes has been well characterized for different lipid systems (26–28), the observed modulation of the kinetics of the conversion of monomeric α-synuclein into amyloid fibrils by different membranes is less well understood (29–32). Most studies of this phenomenon have been performed under conditions of mechanical agitation (32) and/or in the presence of catalyzing polymer surfaces (31), where α-synuclein aggregates also in the absence of lipids and where the mechanism of aggregation has not yet been elucidated. Here, we take a different approach using an experimental procedure with protein-repellant surfaces and under quiescent conditions (33) that enables the systematic study of the manner in which a

Significance

Parkinson's disease is the second most prevalent neurodegenerative disorder and is characterized by the presence in the brains of patients of proteinaceous deposits whose main component is α-synuclein. This protein interacts with membranes as part of its biological function, but this interaction also modulates its kinetics of aggregation. Here, we show that, despite the fact that α-synuclein binds to different types of membranes, it only forms amyloid fibrils in the presence of the most soluble lipids investigated here. This finding is of particular significance because it shows that modifications of the chemical properties of lipids, such as those associated with oxidation and ageing, could be a key determinant of the switch between functional and deleterious interactions between α-synuclein and membranes.

Author contributions: C.G. and C.M.D. designed research; C.G., J.W.P.B., M.M.O., and P.F. performed experiments; C.G., M.V., A.K.B., E.S., and C.M.D. analyzed data; and C.G., J.W.P.B., M.M.O., P.F., M.V., A.K.B., E.S., and C.M.D. wrote the paper.

The authors declare no conflict of interest.

This article is a PNAS Direct Submission.

Freely available online through the PNAS open access option.

[1]Present address: Institute of Physical Biology, University of Düsseldorf, 40225 Duesseldorf, Germany.

[2]To whom correspondence should be addressed. Email: cmd44@cam.ac.uk.

This article contains supporting information online at www.pnas.org/lookup/suppl/doi:10.1073/pnas.1601899113/-/DCSupplemental.

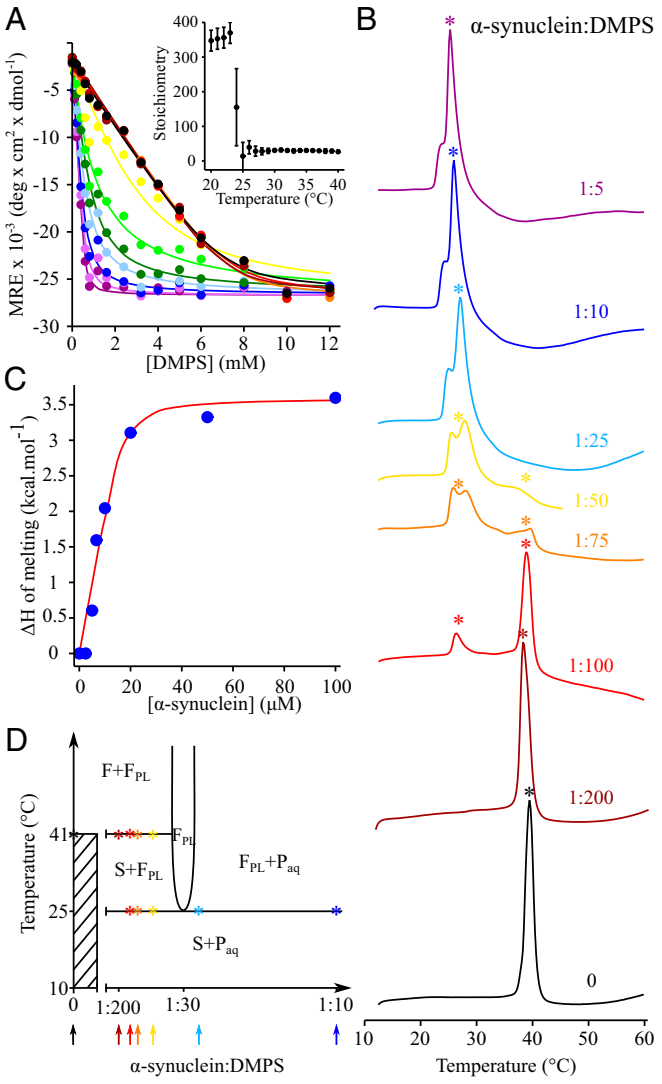

Fig. 1. The interplay between the properties of DMPS model membranes and the lipid-binding properties of α-synuclein at different temperatures. (*A*) Change in the mean residue ellipticity (MRE) measured at 222 nm of α-synuclein (20 μM) incubated in the presence of increasing concentrations of DMPS at 20 °C (black), 21 °C (dark red), 22 °C (red), 23 °C (orange), 24 °C (yellow), 25 °C (light green), 26 °C (green), 27 °C (light blue), 28 °C (dark blue), 29 °C (light purple), and 30 °C (dark purple). (*Inset*) Change in the stoichiometry, the number of DMPS molecules associated with one molecule of α-synuclein (*L*), with temperature. (*B*) DSC thermograms of 500 μM DMPS in the absence (black) and the presence of 2.5 μM (dark red), 5 μM (red), 6.7 μM (orange), 10 μM (yellow), 20 μM (light blue), 50 μM (dark blue), and 100 μM α-synuclein (dark purple). (*C*) Variation of the enthalpy of the transition at 25 °C with increasing concentration of α-synuclein. The experimental values of the change in enthalpy (filled blue circles) were determined by integrating the area below the transition at 25 °C and were then fitted (red line) to a one-step binding model using *SI Appendix*, Eq. **S5** (see the *SI Appendix* for details). (*D*) Proposed phase diagram for the DMPS-protein bilayer phases in an excess aqueous solution (that is metastable for at least 1 h against aggregation). The *x* axis refers to the total composition of the sample (bilayer phases + excess solution), and the composition of the bilayer phase can be determined from the CD data (Fig. 1*A*). Asterisks indicate the temperatures at which the melting transition(s) were observed in the DSC thermograms measured at different P:L ratios. The solid lines are based on the DSC and CD experimental data together with thermodynamic consideration to fulfill the Gibbs phase rule (35). The phase diagram does not account for the partitioning of the excess peptide between the aqueous solution and the lipid phases. F and S refer to the liquid crystalline and solid gel lamellar phases, respectively. F_{PL} refers to the fluid protein–lipid phase. The protein monomer in solution is referred to as P_{aq}. In addition, the diagram does not account for the splitting of the excess heat capacity peak at ~25 °C in the DSC traces because we cannot distinguish the different enthalpic contributions related to protein adsorption, protein conformational change, and lipid melting that may occur simultaneously or sequentially.

change in lipid properties can affect the ability of a model membrane to initiate α-synuclein aggregation. Indeed, we have previously shown that the presence of model membranes composed of 1,2-dimyristoyl-*sn*-glycero-3-phospho-L-serine (DMPS) triggers the aggregation of α-synuclein by specifically enhancing the rate of primary nucleation (33). In addition, this study showed how the protein:lipid (P:L) ratio modulates the kinetics of α-synuclein aggregation in the presence of DMPS; at low P:L ratios, effectively all of the protein molecules are adsorbed onto the surface of the membrane in a thermodynamically stable α-helical state and no aggregation is observed. At high P:L ratios, however, the protein molecules populate both the free monomeric state and the membrane-bound state, leading to rapid amyloid formation (33).

In the present study, we have applied this experimental procedure to probe how changes in the chemical (charge and solubility) and physical (thermotropic) properties of lipids affect the binding of α-synuclein and the magnitude by which model membranes can trigger α-synuclein aggregation. The results reveal that the efficiency of the binding of α-synuclein to model membranes is correlated with their fluidity and, conversely, that the self-assembly of the lipids is affected by their association with the protein. In addition, although α-synuclein has a high affinity for all of the fluid anionic model membranes investigated here, this interaction is not sufficient for the efficient induction of aggregation. Rather, the rate of amyloid fibril formation is shown to be inversely correlated with the free energy of transfer of the lipid molecule from water into the bilayer. These results indicate that the chemical properties of the lipids are likely to play an important role in perturbing the balance between functional and deleterious interactions of α-synuclein with membranes.

Results

Interplay Between the Fluidity of the DMPS Membrane and the Binding Properties of α-Synuclein. To understand the interplay between membrane fluidity and the lipid-binding properties of α-synuclein, we studied the binding of the protein to model membranes composed of DMPS, at temperatures ranging from 20 to 50 °C, by monitoring the conformational change of the protein upon membrane association, using circular dichroism (CD) spectroscopy (Fig. 1*A*). The binding curves are all well described by a one-step binding model (33) (see *Materials and Methods* and the *SI Appendix* for details), enabling the binding affinities and the stoichiometry, the number of lipid molecules associated with a given molecule of α-synuclein (*L*), to be determined at each temperature (Fig. 1*A*, *Inset*). We found that the stoichiometry dropped tenfold, from more than 350 at temperatures below 23 °C to ca. 30 at temperatures above 25 °C (Fig. 1*A*, *Inset*).

In the light of this dramatic and abrupt change in stoichiometry at 23–25 °C, we then investigated how the binding of α-synuclein to DMPS model membranes could affect their thermotropic properties using differential scanning calorimetry (DSC) (Fig. 1*B*). In the absence of protein, the thermogram of DMPS is characterized by a sharp transition centered at 41 °C, which corresponds to the conversion of the membrane from a gel phase bilayer with solid hydrocarbon chains (S) to a liquid crystalline bilayer with fluid hydrocarbon chains (F) (34). When α-synuclein is added to the sample, a second broad peak at ca. 23–29 °C appears in the thermogram. As the ratio of [α-synuclein]:[DMPS] increases, the enthalpy of the high-temperature melting transition, as obtained from the integration of the area under the corresponding heat capacity peak, decreases, whereas that associated with the low-temperature transition increases. These two transitions can be attributed to the existence of two distinct lipid populations: one transition corresponds to that of protein-free lipids, whose melting

temperature is 41 °C, and the other to that of lipids closely associated with the protein, whose melting temperature is reduced and centered at 25 °C. We then analyzed the enthalpy of melting of the DMPS molecules associated with the protein with increasing concentrations of α-synuclein (Fig. 1*C*). The total change in enthalpy measured at the lower temperature originates from several simultaneous processes (protein binding and folding as well as lipid melting) and is to a first approximation proportional to the number of lipid molecules involved in interactions with α-synuclein molecules (see the *SI Appendix* for details) (Fig. 1*C*). The resulting values for the K_D and stoichiometry (0.8 μM and 29, respectively) obtained from a fit to the DSC data agree well with those obtained from the binding of the protein to the fluid phase obtained from CD measurements (0.5 μM and 31, respectively) (Table 1). This result suggests that the one-step binding model used in this study provides a consistent and quantitative description of the changes in the fraction of either protein bound to lipid or lipid bound to protein (depending on the experimental observable) for the different P:L ratios used in our experiments.

In Fig. 1*D*, we propose a phase diagram that is consistent with the DSC and CD experiments and that fulfils the formal requirements set by the Gibbs phase rule (35). The phases include the fluid (F) and solid gel (S) phases of the lipid, a fluid protein–lipid phase (F_{PL}) with a close to constant P:L ratio over the whole temperature range, and the solution containing unbound protein monomers (P_{aq}). The horizontal lines on the phase diagram at 25 and 41 °C correspond to the melting transitions of the protein–lipid (PL) complex and pure DMPS, respectively, as observed in the DSC scans of DMPS measured for different P:L ratios (Fig. 1*B*). The vertical line is drawn at P:L = 1:30, with 30 being the stoichiometry at which DMPS in its fluid phase binds to α-synuclein, as determined using CD (Fig. 1*A*, *Inset*). Each DSC scan of DMPS measured at a given P:L ratio corresponds to a vertical cut of the phase diagram at the same P:L ratio, as indicated by the arrows in Fig. 1*D*. In the absence of protein (i.e., P:L = 0), DMPS molecules form a solid gel phase below 41 °C and a fluid phase at higher temperatures. For α-synuclein:DMPS ratios below ca. 1:30 (brown, red, orange, and yellow DSC thermograms and arrows in Fig. 1 *B* and *D*, respectively) and temperatures below 25 °C, however, all of the DMPS molecules form a solid gel phase with only a small number of protein molecules adsorbed onto the surface. At 25 °C, more protein molecules adsorb onto the membrane, and the DMPS molecules associated with α-synuclein monomers melt, resulting in the formation of the F_{PL} phase. As long as α-synuclein:DMPS ratios are below 1:30, there are insufficient protein molecules in solution to convert all of the DMPS molecules into the protein/lipid F_{PL} phase. The remaining protein-free DMPS molecules then form a solid gel phase and melt when the temperature reaches 41 °C. For P:L ratios above 1:30 (blue line in Fig. 1 *B* and *D*) and for temperatures below 25 °C, all DMPS molecules form a solid gel phase with a small number of protein molecules adsorbed at the surface. When the temperature reaches 25 °C, there are enough protein molecules in solution to enable all DMPS molecules to form the protein/lipid F_{PL} phase.

Taken together, these results show that the fluidity of DMPS membranes affects the binding properties of α-synuclein and, conversely, that the binding of the protein to DMPS membranes affects its lipid phase behavior.

α-Synuclein Binds Preferentially to Fluid Membranes. As a second complementary approach to study the effect of a change in the membrane fluidity on the lipid-binding of α-synuclein, we chose to study the behavior of the protein in the presence of model membranes composed of lipids with the same head group, phosphatidylserine (PS), but with hydrocarbon chains differing in their lengths and degrees of unsaturation (Table 1). The melting temperatures of these lipids are expected to increase with the lengths of the hydrocarbon chains [T_m (1,2-dilauroyl-*sn*-glycero-3-phospho-L-serine) (DLPS) < T_m (DMPS) < T_m (1,2-dipalmitoyl-*sn*-glycero-3-phospho-L-serine) (DPPS)] and decrease with their degree of unsaturation [T_m (1,2-dioleoyl-*sn*-glycero-3-phospho-L-serine) (DOPS) < T_m (1-palmitoyl-2-oleoyl-*sn*-glycero-3-phospho-L-serine) (POPS) < T_m (DPPS)] (36, 37). The DSC traces for these lipids show melting transitions centered at 14, 41, and 55 °C for DLPS, DMPS, and DPPS, respectively, values in good agreement with those reported in the literature (11) (Fig. 2*A*). On the addition of an excess of α-synuclein, we observed, as for DMPS [Fig. 1*B* and previous studies (33)], that the melting temperatures of DPPS and DLPS were decreased (Fig. 2*A*), as a result of the binding of the protein to the membrane.

To characterize the specific effects of a change in the fluidity on the binding of α-synuclein to model membranes, we chose to carry out studies at 30 °C. At this temperature, our DSC data indicates that DOPS, POPS, DLPS, and DMPS all form a fluid F_{PL} phase, whereas DPPS forms a solid gel phase in the presence of an excess of protein (Fig. 2*A*). Fig. 2*B* shows the binding curves of α-synuclein to the model membranes composed of the different lipids, monitored using CD, and in each case the binding data are again all well-described by the one-step binding model (values of K_D and L were estimated from the fits to this model; Table 1). Although the affinities of α-synuclein to these model membranes were found to be very similar, within error, the number of lipid molecules associated with each molecule of α-synuclein was observed to vary from ∼30 for model membranes in the fluid phase at 30 °C (DLPS, DMPS, POPS, DOPS) to over 250 for those in a solid gel phase (DPPS) at the same temperature (Table 1). The differences in stoichiometries observed for membranes in the fluid phase and in the solid gel phase can be attributed to the differences in the properties of the lipids involved, in particular the higher degree of exposure of hydrophobic regions (A_1) (Table 1 and Fig. 2*C*) and the higher lateral diffusion in the fluid bilayer. Taken together, these results suggest that α-synuclein interacts more favorably with membranes in the fluid phase than in the gel phase, as reflected by the much more favorable stoichiometry.

The Aggregation of α-Synuclein Is Triggered in the Presence of Model Membranes Composed of Lipids with Short Saturated Hydrocarbon Chains. Our results show that the fluidity of the anionic membrane is essential for efficient binding of α-synuclein. We then investigated

Table 1. Structural parameters and biophysical properties of DOPS, POPS, DLPS, DMPS, and DPPS

Lipid parameters	DOPS	POPS	DLPS	DMPS	DPPS
Acyl chain	$(18:1)_2$	16:0/18:1	$(12:0)_2$	$(14:0)_2$	$(16:0)_2$
Area per lipid, Å*	65.3	55	58	55.6†	44.2
T_m (free), °C	<10	17	14	41	55
T_m (α-synuclein–bound), °C	<10	<10	<10	25–28	45
Phase at 30 °C	Fluid	Fluid	Fluid	Fluid	Gel
K_D (30 °C), μM	0.2 ± 0.1	0.4 ± 0.2	0.3 ± 0.1	0.5 ± 0.2	0.1 ± 0.7
L (30 °C)	33 ± 1	32 ± 2	28 ± 1	31 ± 2	251 ± 62

*Data are from ref. 49.
†Calculated value (see the *SI Appendix* for details).

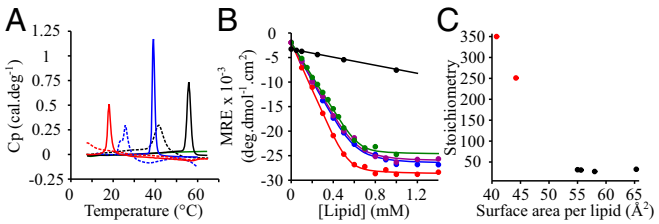

Fig. 2. Lipid-binding properties of α-synuclein in the presence of model membranes composed of lipids with different chain properties. (*A*) DSC thermograms of 500 μM DMPS (blue), DLPS (red), DOPS (green), and DPPS (black) in the absence (continuous lines) and presence (dotted lines) of 100 μM α-synuclein. (*B*) Change in the mean residual ellipticity (MRE) at 222 nm of α-synuclein (20 μM) incubated at 30 °C in the presence of increasing concentrations of DOPS (green), POPS (purple), DLPS (red), DMPS (blue), and DPPS (black). (*C*) Variation in the number of lipid molecules associated with one molecule of α-synuclein as a function of the surface area of the different lipids. The data points colored in red and black correspond to model membranes in the solid gel and fluid phase, respectively.

how a change in the lipid properties can affect the magnitude by which the model membranes are able to promote α-synuclein aggregation. First, α-synuclein was incubated at 30 °C under quiescent conditions in the presence of 100 μM DOPS, POPS, DLPS, DMPS, and DPPS model membranes. As we observed previously, the presence of DMPS was found to promote the formation of amyloid fibrils by α-synuclein (33). Similarly, DLPS was observed to trigger fibril formation, indeed to an even greater degree than is the case with DMPS (Fig. 3*A*). We found that the fibrils formed by α-synuclein in the presence of DLPS and DMPS share the same morphological properties (Fig. 3*C* and ref. 33), and the concentration of fibrils formed under these conditions is proportional to the initial concentration of lipid rather than protein molecules (Fig. 3*B* and *SI Appendix*, Fig. S1). By contrast, α-synuclein was not found to form amyloid fibrils at an enhanced rate relative to bulk aqueous solution in the presence of the other model membranes in the fluid state that were investigated here (DOPS and POPS), nor for those in the solid gel phase (DPPS) (Fig. 3*A*) at 30 °C. In addition, we incubated α-synuclein in the presence of model membranes composed of 1,2-dioleoyl-*sn*-glycero-3-phosphoethanolamine (DOPE):DOPS:1,2-dioleoyl-*sn*-glycero-3-phosphocholine (DOPC) (50:30:20), a lipid composition suggested to mimic closely that of synaptic vesicles (38), but again we observed no significant degree of amyloid formation under these conditions. The same observation was made when α-synuclein was incubated in the presence of model membranes consisting of DOPE:DOPS:DOPC (50:30:20) containing increasing concentrations of cholesterol (10–40%), indicating that the presence of cholesterol does not itself initiate α-synuclein aggregation under these conditions. These results suggest that α-synuclein aggregation is triggered efficiently by model membranes composed of lipids with short saturated hydrocarbon chains. Moreover, the rate of aggregation was found to be significantly faster with the shorter chain DLPS compared with that of DMPS (Fig. 3*A*). In addition, α-synuclein was incubated in the presence of DPPS model membranes at 50 °C, a temperature at which the phase of these membranes is the same as that of DMPS membranes at 30 °C, and we did not observe promotion of amyloid formation. This result suggests that the chemical nature of the lipid molecules, rather than their phase state, influences the magnitude by which α-synuclein aggregation is initiated by the model membranes.

Finally, we studied whether or not the formation or presence of lipid domains can trigger the initiation of α-synuclein aggregation. The binding and aggregation properties of α-synuclein were therefore investigated in the presence of model membranes prepared from an equimolar mixture of DLPS and DPPS at 30 °C. At this temperature, DLPS forms a fluid phase, whereas DPPS forms a solid gel phase, and model membranes composed of these two lipids are expected to have a heterogeneous phase. Indeed, the DSC thermogram of mixed DLPS:DPPS (50:50) model membranes is characterized by the presence of multiple broad peaks (Fig. 4*A*), suggesting the coexistence of DLPS-rich fluid and DPPS-rich solid gel phases at temperatures between 25 and 50 °C, in agreement with a previous published DSC study of mixed DLPC:DPPC model membranes (39). We then compared the binding properties of α-synuclein to these model membranes using CD and found that the number of lipid molecules associated with a molecule of α-synuclein in the mixed DLPS:DPPS model membranes was twice that in the pure DLPS model membranes, suggesting that the protein interacts essentially with DLPS lipids at the surface of DLPS:DPPS model membranes (Fig. 4*B*) (K_D = 0.10 ± 0.03 μM; L = 49 ± 2). Finally, we incubated α-synuclein in the presence of these mixed DLPS:DPPS (50:50, M:M, 100 μM) model membranes at 30 °C and observed the formation of fibrils, albeit at a much lower rate than that observed in the presence of a molar equivalent of DLPS model membranes (50 μM) and a much faster rate than that observed in the presence of DPPS, where no significant aggregation is detected within the time frame of the experiments. These results suggest that the presence of DLPS as a lipid component rather than the presence of segregated domains in the model membranes is required to trigger the formation of amyloid fibrils by α-synuclein. An important additional finding is that the charge density of the model membranes affects both the lipid binding of α-synuclein and the ability of these model membranes to trigger α-synuclein aggregation (*SI Appendix*, Fig. S2). Indeed, the binding of α-synuclein to 1,2-dimyristoyl-*sn*-glycero-3-phosphocholine (DMPC):DMPS model membranes was shown to decrease as the fraction of DMPC increases relative to that of DMPS (*SI Appendix*, Fig. S2*A*). In addition, we observed that DMPC:DMPS model membranes did not detectably stimulate the aggregation of α-synuclein for DMPC:DMPS ratios above 25:75, an observation that can be attributed to the fact that the binding between the protein and the model membranes is greatly reduced (*SI Appendix*, Fig. S2*B*). These results are consistent with previous observations that the binding affinity of α-synuclein to negatively charged DMPS model membranes decreases at higher ionic strength where the electrostatic interactions between the protein and the negative charge of the PS head groups are screened (33).

Discussion

The binding of α-synuclein to negatively charged membranes has been suggested to involve the adsorption of the protein onto the surface of the membranes, driven by electrostatic interactions, accompanied by the formation of an extended N-terminal α-helical region located at the polar head groups of the lipids, promoting interactions between the hydrophobic face of the protein and the hydrophobic region of the lipid molecules (16, 23). In this study, we describe how the binding of α-synuclein to negatively charged membranes induces lipid segregation into protein-poor

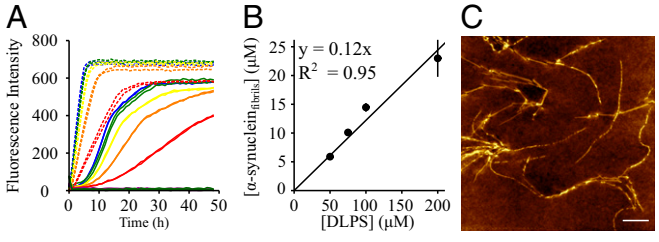

Fig. 3. Aggregation propensity of α-synuclein in the presence of model membranes composed of lipids with different chain properties. (*A*) Evolution of ThT fluorescence when 20 μM (red), 40 μM (orange), 60 μM (yellow), 80 μM (green) and 100 μM (blue) α-synuclein was incubated in the presence of 100 μM DLPS (dashed line) or DMPS (solid line) and when 100 μM α-synuclein was incubated in the presence of 100 μM DOPS (dark green), POPS (dark purple), or DPPS (black). (*B*) Dependence of the concentration of fibrils formed by α-synuclein at the plateau phase on the initial concentration of DLPS. (*C*) Atomic force microscopy image of α-synuclein fibrils formed after incubation of 100 μM α-synuclein in the presence of 100 μM DLPS. (White scale bar, 1 μm.)

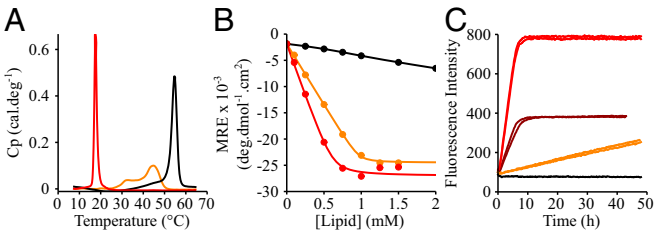

Fig. 4. Effect of the presence of mixed phases within the membrane on the lipid-binding of α-synuclein and the kinetics of amyloid formation. (*A*) DSC thermograms of 500 μM DLPS (red), DPPS (black), and DLPS:DPPS (50:50, M:M) (orange) model membranes. (*B*) Change in the mean residual ellipticity at 222 nm of α-synuclein (20 μM) incubated at 30 °C in the presence of increasing concentrations of model membranes made with DLPS (red) or DPPS (black) or an equimolar mixture of DLPS and DPPS (DLPS:DPPS, 50:50, M:M) (orange). (*C*) Evolution of the ThT fluorescence signal when 100 μM α-synuclein was incubated in the presence of 50 μM DLPS (brown) and 100 μM DLPS (red), DPPS (black), and DLPS:DPPS (50:50, M:M) (orange) model membranes.

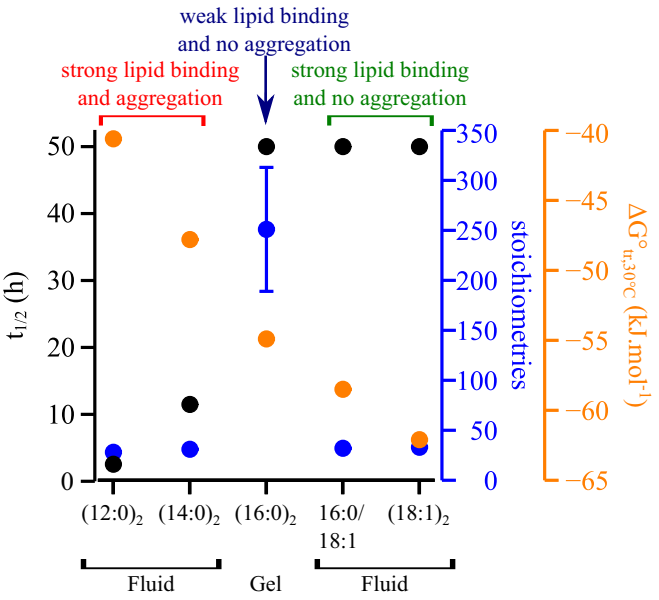

Fig. 5. Physical and chemical properties of the lipids influence the binding efficiency and the aggregation propensity of α-synuclein in the presence of model membranes. The energy of transfer of a lipid molecule from water to a bilayer ($\Delta G°_{tr,30\ °C}$) (orange), the stoichiometry of α-synuclein:lipid binding (blue), and the half-time for the aggregation of α-synuclein (black) are plotted for each lipid system: DLPS [(12:0)$_2$], DMPS [(14:0)$_2$], DPPS [(16:0)$_2$], POPS (16:0/18:1), and DOPS [(18:1)$_2$]. The phase of each lipid systems in the presence of an excess of protein at 30 °C is indicated below the *x* axis.

and protein-rich populations whose melting temperatures are 41 and ∼25 °C, respectively. Although the binding of peripheral proteins to membranes can induce a progressive change in their T_m value with increasing protein concentration (12, 13), such a segregation of lipids into populations with distinct properties has previously also been observed for the antimicrobial peptide peptidyl-glycylleucine-carboxyamide (PGLa) binding to negatively charged model membranes [1,2-dimyristoyl-*sn*-glycero-3-phospho-(1′-rac-glycerol) (DMPG), 1,2-dipalmitoyl-*sn*-glycero-3-phospho-(1′-rac-glycerol) (DPPG) and 1,2-distearoyl-*sn*-glycero-3-phospho-(1′-rac-glycerol) (DSPG)], which in that case led to the formation of a phase with higher T_m because of the stabilization of an interdigitated gel phase (40). By contrast, our CD and DSC results suggest that α-synuclein binding stabilizes the fluid phase formed by negatively charged lipids.

Our results show that the binding affinity of α-synuclein to model membranes is highest when the latter adopt a fluid phase (Fig. 5) because such membranes expose on average more hydrophobic area than do those in the solid gel phase (Fig. 2*C*). The fluidity of the membrane is therefore considered essential for efficient binding of α-synuclein, but this property does not determine the magnitude by which the aggregation of α-synuclein is promoted. Indeed, despite the fact that α-synuclein binds with similar affinities to model membranes composed of different negatively charged phospholipids, we have shown that the aggregation of the protein is enhanced only in the presence of lipids with the shortest hydrocarbon chains (Fig. 5). In particular, our results show that α-synuclein binds to model membranes composed of lipids commonly found in the membrane of synaptic vesicles such as DOPE, DOPC, DOPS, POPS, and cholesterol (38) but that these lipids do not enhance dramatically the aggregation of the protein under the conditions used in this study, even if incubated for several days under quiescent conditions. The binding of the protein to DMPS and DLPS model membranes however substantially enhances its aggregation rate, with the kinetics of amyloid formation being faster for DLPS, which has a shorter chain length than does DMPS. Interestingly, the standard change in free energy of transfer of a lipid molecule from water into a bilayer (a measure for its solubility in water) correlates strongly with the length of its lipid hydrocarbon chain(s) (11). Our results show that only lipids that have the highest solubility in aqueous solution [ca. 100 and 10 nM for DLPS and DMPS, respectively (11)] trigger α-synuclein aggregation (Fig. 5).

This finding might be of physiological relevance because of the observation that lipids with short hydrocarbon chains can result from the peroxidation of polyunsaturated lipids (41, 42), a phenomenon shown to be highly damaging to cells and associated with the modification of the fluidity of the membrane. Moreover, the shorter and more soluble lipids are more readily transported to other organelles via membrane trafficking (41, 42). Interestingly, another family of lipids, the gangliosides, in particular GM1 and GM3, have also been shown to accelerate the kinetics of amyloid formation by α-synuclein (43) and other amyloidogenic systems such as the Aβ peptide, the aggregation of which is the hallmark of Alzheimer's disease (44). These lipids have the characteristic feature of a large polar head that can increase their solubility in aqueous solution (1–30 μM for GM1) (11, 45, 46). It is interesting in this regard that the presence of transmembrane and peripheral proteins in synaptic vesicles is also likely to modulate the efficiency of α-synuclein binding to the vesicles, and hence their capacity to enhance protein aggregation (38, 47).

Based on these results, it appears likely that the membranes not only represent an interface that favors a high local concentration of α-synuclein molecules, hence accelerating the nucleation step, but also play a more active role in the aggregation process. The finding that the kinetics of aggregation correlate with the solubility of the lipid molecules suggests that at least part of the free energy barrier for the aggregation process is related to the transfer of lipid molecules from a membrane to a protein environment.

Taken together, these findings suggest that the fluidity of the membrane plays a role in α-synuclein lipid binding process but not in the initiation of α-synuclein aggregation. The chemical properties of the lipids, however, and in particular their solubility, determine the magnitude by which the model membranes trigger α-synuclein aggregation and are likely to play a crucial role in the balance between functional and deleterious interactions of α-synuclein with biological membranes.

Materials and Methods

Materials. DMPS (sodium salt), DMPC, DOPS (sodium salt), DOPE, DOPC, POPS (sodium salt), DLPS (sodium salt), DPPS (sodium salt), and cholesterol (ovine wool; ≥98%) were purchased from Avanti Polar Lipids. Sodium phosphate monobasic (NaH_2PO_4; ≥99.0%; BioPerformance Certified), sodium phosphate dibasic (Na_2HPO_4; ≥99.0%; ReagentPlus), and sodium azide (NaN_3; ≥99.5%) were purchased from Sigma Aldrich. Thioflavin T UltraPure Grade (ThT) (≥95%) was purchased from Eurogentec.

Protein and Lipid Dispersion Preparation. Wild-type α-synuclein was expressed and purified as described previously (48). The lipid dispersions were prepared as described previously using sonication (see the *SI Appendix* for more details) (33).

CD. CD samples were prepared by incubating 20 μM α-synuclein in the presence of increasing concentrations of lipid in 20 mM phosphate buffer (pH 6.5). Far-UV CD spectra were recorded on a JASCO J-810 equipped with a Peltier thermally controlled cuvette holder at 30 °C (see the *SI Appendix* for more details). The CD data were analyzed as previously described (33) (see the *SI Appendix* for details).

Differential Scanning Calorimetry. The thermograms were acquired using a Microcal VP-DSC calorimeter (Malvern Instruments) with a scanning rate of 1 °C min^{-1} from 5 to 65 °C. Protein and lipid samples were degassed for 20 min at room temperature before mixing and acquisition of the DSC thermograms. All of the DSC thermograms reported in this article were corrected by subtracting the thermogram of the phosphate buffer and correspond to the first scan, unless otherwise stated (see the *SI Appendix* for the details of the analysis).

α-Synuclein Aggregation in the Presence of Model Membranes. α-Synuclein was incubated in 20 mM sodium phosphate, pH 6.5, in the presence of 50 μM ThT (Sigma) and increasing concentrations of lipid. The change in the ThT fluorescence signal with time was monitored using a plate reader (BMG Labtech) under quiescent conditions at 30 °C if not stated otherwise. Corning 96-well plates with half-area (3881, polystyrene, black with clear bottom) nonbinding surfaces were used for all experiments. At the end of each aggregation experiment, the concentrations of fibrils formed were determined as described previously (33). The half-times plotted in Fig. 5 correspond to the times at which the ThT fluorescence signal is half the signal at the plateau of the aggregation curve of α-synuclein in the presence of DMPS and DLPS. For POPS, DOPS, and DPPS, the lower bound of the half-time is indicated and corresponds to the incubation time of α-synuclein with these lipid systems used in our study during which the aggregation of the protein was not observed (i.e., 50 h).

ACKNOWLEDGMENTS. We thank Tuomas Knowles, Christopher Waudby, and John Christodoulou for valuable discussions. This work was supported by the UK Biotechnology and Biological Sciences Research Council (BBSRC) (C.M.D., M.V., and M.M.O.); the Wellcome Trust (C.M.D. and M.V.); Magdalene College, Cambridge (A.K.B.); the Leverhulme Trust (A.K.B.); the Boehringer Ingelheim Fonds (P.F.); the Swedish Research Council (E.S.); and the Cambridge Centre for Misfolding Disease (C.M.D., M.V., J.W.P.B., P.F., and C.G.).

1. Cabin DE, et al. (2002) Synaptic vesicle depletion correlates with attenuated synaptic responses to prolonged repetitive stimulation in mice lacking α-synuclein. *J Neurosci* 22(20):8797–8807.
2. Lee HJ, Choi C, Lee SJ (2002) Membrane-bound α-synuclein has a high aggregation propensity and the ability to seed the aggregation of the cytosolic form. *J Biol Chem* 277(1):671–678.
3. Goedert M (2001) α-synuclein and neurodegenerative diseases. *Nat Rev Neurosci* 2(7): 492–501.
4. Chiti F, Dobson CM (2006) Protein misfolding, functional amyloid, and human disease. *Annu Rev Biochem* 75:333–366.
5. Ouberai MM, et al. (2013) α-Synuclein senses lipid packing defects and induces lateral expansion of lipids leading to membrane remodeling. *J Biol Chem* 288(29): 20883–20895.
6. Middleton ER, Rhoades E (2010) Effects of curvature and composition on α-synuclein binding to lipid vesicles. *Biophys J* 99(7):2279–2288.
7. Garten M, et al. (2015) Methyl-branched lipids promote the membrane adsorption of α-synuclein by enhancing shallow lipid-packing defects. *Phys Chem Chem Phys* 17(24): 15589–15597.
8. Epand RM (1998) Lipid polymorphism and protein-lipid interactions. *Biochim Biophys Acta* 1376(3):353–368.
9. van Meer G, Voelker DR, Feigenson GW (2008) Membrane lipids: where they are and how they behave. *Nat Rev Mol Cell Biol* 9(2):112–124.
10. Engelman DM (2005) Membranes are more mosaic than fluid. *Nature* 438(7068): 578–580.
11. Marsh D (2013) *Handbook of Lipid Bilayers* (CRC Press, Boca Raton, FL).
12. Papahadjopoulos D, Moscarello M, Eylar EH, Isac T (1975) Effects of proteins on thermotropic phase transitions of phospholipid membranes. *Biochim Biophys Acta* 401(3):317–335.
13. McElhaney RN (1982) The use of differential scanning calorimetry and differential thermal analysis in studies of model and biological membranes. *Chem Phys Lipids* 30(2-3):229–259.
14. Drin G, Antonny B (2010) Amphipathic helices and membrane curvature. *FEBS Lett* 584(9):1840–1847.
15. Drin G, et al. (2007) A general amphipathic alpha-helical motif for sensing membrane curvature. *Nat Struct Mol Biol* 14(2):138–146.
16. Antonny B (2011) Mechanisms of membrane curvature sensing. *Annu Rev Biochem* 80: 101–123.
17. Bhatia VK, Hatzakis NS, Stamou D (2010) A unifying mechanism accounts for sensing of membrane curvature by BAR domains, amphipathic helices and membrane-anchored proteins. *Semin Cell Dev Biol* 21(4):381–390.
18. Cui H, Lyman E, Voth GA (2011) Mechanism of membrane curvature sensing by amphipathic helix containing proteins. *Biophys J* 100(5):1271–1279.
19. Vamparys L, et al. (2013) Conical lipids in flat bilayers induce packing defects similar to that induced by positive curvature. *Biophys J* 104(3):585–593.
20. Vanni S, Hirose H, Barelli H, Antonny B, Gautier R (2014) A sub-nanometre view of how membrane curvature and composition modulate lipid packing and protein recruitment. *Nat Commun* 5:4916.
21. Vanni S, et al. (2013) Amphipathic lipid packing sensor motifs: probing bilayer defects with hydrophobic residues. *Biophys J* 104(3):575–584.
22. Hatzakis NS, et al. (2009) How curved membranes recruit amphipathic helices and protein anchoring motifs. *Nat Chem Biol* 5(11):835–841.
23. Jao CC, Hegde BG, Chen J, Haworth IS, Langen R (2008) Structure of membrane-bound α-synuclein from site-directed spin labeling and computational refinement. *Proc Natl Acad Sci USA* 105(50):19666–19671.
24. Hellstrand E, et al. (2013) Adsorption of α-synuclein to supported lipid bilayers: positioning and role of electrostatics. *ACS Chem Neurosci* 4(10):1339–1351.
25. Pfefferkorn CM, et al. (2012) Depth of α-synuclein in a bilayer determined by fluorescence, neutron reflectometry, and computation. *Biophys J* 102(3):613–621.
26. Eliezer D, Kutluay E, Bussell R, Jr, Browne G (2001) Conformational properties of α-synuclein in its free and lipid-associated states. *J Mol Biol* 307(4):1061–1073.
27. Bodner CR, Dobson CM, Bax A (2009) Multiple tight phospholipid-binding modes of α-synuclein revealed by solution NMR spectroscopy. *J Mol Biol* 390(4):775–790.
28. Fusco G, et al. (2014) Direct observation of the three regions in α-synuclein that determine its membrane-bound behaviour. *Nat Commun* 5:3827.
29. Fink AL (2006) The aggregation and fibrillation of α-synuclein. *Acc Chem Res* 39(9): 628–634.
30. Martinez Z, Zhu M, Han S, Fink AL (2007) GM1 specifically interacts with α-synuclein and inhibits fibrillation. *Biochemistry* 46(7):1868–1877.
31. Grey M, Linse S, Nilsson H, Brundin P, Sparr E (2011) Membrane interaction of α-synuclein in different aggregation states. *J Parkinsons Dis* 1(4):359–371.
32. Zhu M, Li J, Fink AL (2003) The association of alpha-synuclein with membranes affects bilayer structure, stability, and fibril formation. *J Biol Chem* 278(41):40186–40197.
33. Galvagnion C, et al. (2015) Lipid vesicles trigger α-synuclein aggregation by stimulating primary nucleation. *Nat Chem Biol* 11(3):229–234.
34. Sturtevant JM (1987) Biochemical applications of differential scanning calorimetry. *Annu Rev Phys Chem* 38:463–488.
35. Evans DF, Wennerström H (1999) *The Colloidal Domain: Where Physics, Chemistry, Biology, and Technology Meet* (Wiley-VCH, New York).
36. Mason JT, Huang CH (1981) Chain length dependent thermodynamics of saturated symmetric-chain phosphatidylcholine bilayers. *Lipids* 16(8):604–608.
37. Brenner RR (1984) Effect of unsaturated acids on membrane structure and enzyme kinetics. *Prog Lipid Res* 23(2):69–96.
38. Takamori S, et al. (2006) Molecular anatomy of a trafficking organelle. *Cell* 127(4): 831–846.
39. Seeger HM, Fidorra M, Heimburg T (2005) Domain size and fluctuations at domain interfaces in lipid mixtures. *Macromol Symp* 219(1):85–96.
40. Pabst G, et al. (2008) Membrane thickening by the antimicrobial peptide PGLa. *Biophys J* 95(12):5779–5788.
41. Beranova L, Cwiklik L, Jurkiewicz P, Hof M, Jungwirth P (2010) Oxidation changes physical properties of phospholipid bilayers: fluorescence spectroscopy and molecular simulations. *Langmuir* 26(9):6140–6144.
42. Negre-Salvayre A, et al. (2010) Pathological aspects of lipid peroxidation. *Free Radic Res* 44(10):1125–1171.
43. Grey M, et al. (2015) Acceleration of α-synuclein aggregation by exosomes. *J Biol Chem* 290(5):2969–2982.
44. Matsuzaki K (2014) How do membranes initiate Alzheimer's Disease? Formation of toxic amyloid fibrils by the amyloid β-protein on ganglioside clusters. *Acc Chem Res* 47(8):2397–2404.
45. Rauvala H (1979) Monomer-micelle transition of the ganglioside GM1 and the hydrolysis by Clostridium perfringens neuraminidase. *Eur J Biochem* 97(2):555–564.
46. Corti M, Degiorgio V, Ghidoni R, Sonnino S, Tettamanti G (1980) Laser-light scattering investigation of the micellar properties of gangliosides. *Chem Phys Lipids* 26(3):225–238.
47. Wilhelm BG, et al. (2014) Composition of isolated synaptic boutons reveals the amounts of vesicle trafficking proteins. *Science* 344(6187):1023–1028.
48. Hoyer W, et al. (2002) Dependence of α-synuclein aggregate morphology on solution conditions. *J Mol Biol* 322(2):383–393.
49. Petrache HI, et al. (2004) Structure and fluctuations of charged phosphatidylserine bilayers in the absence of salt. *Biophys J* 86(3):1574–1586.

Supporting Information: Chemical properties of lipids strongly affect the kinetics of the membrane-induced aggregation of α-synuclein

Céline Galvagnion[1], James W.P. Brown[1], Myriam M. Ouberai[2], Patrick Flagmeier[1], Michele Vendruscolo[1], Alexander K. Buell[1,3], Emma Sparr [4] and Christopher M. Dobson[1,*]

[1] Department of Chemistry, University of Cambridge, Lensfield Road, Cambridge CB2 1EW, UK
[2] Nanoscience centre, Department of Engineering, University of Cambridge, Cambridge, CB3 0FF, United Kingdom
[3] Present address: Institute of Physical Biology, University of Düsseldorf, Universitätsstr. 1, 40225 Düsseldorf, Germany
[4] Division of Physical Chemistry, Chemistry Department, Lund University , P.O. Box 124, 22100 Lund, Sweden
*author to whom correspondence should be addressed: cmd44@cam.ac.uk

SI Methods

1 Lipid dispersion preparation

The stocks of the lipids were purchased either as solutions or as powder. Lipid films were prepared by transferring the desired volume of lipid stock solution with a Hamilton syringe into a round bottom flask and the solvent was evaporated using a gentle flow of nitrogen gas. The flasks were then incubated for $\geq$ 1 h under vacuum to remove any residual traces of solvent. The lipid films or powders were dissolved in 20 mM phosphate buffer ((Na_2HPO_4/NaH_2PO_4), pH 6.5, 0.01%NaN_3), and stirred at a temperature above their respective melting temperature (T_m) for 2 h. The solutions were then frozen and thawed five times using dry ice and a water bath at a temperature above their T_m values, respectively. Lipid dispersions were prepared using sonication (3 $\times$ 5 min, 50 % cycles, 10 % maximum power) on ice. After centrifugation (13k rpm, 30 min), the sizes of the vesicles were measured with dynamic light scattering (Zetasizer Nano ZSP, Malvern Instruments, Malvern, UK) and found to consist of a distribution centered at 20 nm diameter.

2 Determination of the concentration of fibrils formed by α-synuclein in the presence of model membranes

For each P:L ratios, we incubated two types of samples in the micro-well plate: one that contains ThT and that was used to follow the kinetics of amyloid formation in real time and another that did not contain ThT. The rationale behind this dual incubation is that protein concentrations are easier to determine in the absence of ThT, due to the absorption band that ThT has around 280 nm. Once the increase in ThT fluorescence reached the plateau, we centrifuged (90 krpm, 30 min, 20°C) each reaction mixture which did not contained ThT and determined the concentration of soluble monomeric protein remaining in solution in the supernatant ($[\alpha - synuclein_{supernatant}]$) using absorbance at 275 nm and an extinction coefficient of 5,600. The concentration of aggregates formed ($[\alpha - synuclein_{fibrils}]$) were then calculated using the following equation:

$$[\alpha - synuclein_{fibrils}] = [\alpha - synuclein_{initial}] - [\alpha - synuclein_{supernatant}] \tag{S1}$$

with $[\alpha - synuclein_{initial}]$, the concentration of protein in the reaction mixture at time 0.

3 Circular dichroism

3.1 Data Acquisition

Quartz cuvettes with path lengths of 1 mm were used and CD spectra were obtained by averaging five individual spectra recorded between 250 and 200 nm with a bandwidth of 1 nm, a data pitch of 0.2 nm, a scanning speed of 50 nm/min, and a response time of 1 s. Each value of the CD signal intensity reported at 222 nm corresponds to the average of five measurements, each acquired for 10 s. For each protein sample, the CD signal of the buffer used to solubilize the protein was recorded and subtracted from the CD signal of the protein.

3.2 Data Analysis

The observed CD signal (CD_{obs}) consists of the sum of the signals of the lipid-bound and free α-synuclein:

$$CD_{obs} = x_{\alpha-syn_B} CD_B + x_{\alpha-syn_F} CD_F \tag{S2}$$

where $x_{\alpha-syn_B}$ and $x_{\alpha-syn_F}$ are the fractions of α-synuclein bound to the membrane and free in solution, as implied from the protein conformational change upon membrane association. CD_B and CD_F are the CD signals of the bound and free forms of α-synuclein, respectively. By assuming that $x_{\alpha-syn_B} + x_{\alpha-syn_F} = 1$, and that the signals of α-synuclein in the presence of buffer, or in the presence of model membranes under saturating conditions, correspond to CD_F and CD_B, respectively, the fraction of α-synuclein bound to SUV for each sample can be expressed as:

$$x_{\alpha-syn_B} = \frac{CD_{obs} - CD_F}{CD_B - CD_F} \tag{S3}$$

We used the following model: $\alpha - \text{syn} + \text{lipid}_\text{L} \rightleftharpoons \alpha - \text{syn(lipid)}_\text{L}$, which corresponds to a non-cooperative binding Langmuir-Hill adsorption model, and the following equation to fit the measured CD signal:

$$x_B = \frac{([\alpha - syn] + \frac{[lipid]}{L} + K_D) - \sqrt{([\alpha - syn] + \frac{[lipid]}{L} + K_D)^2 - \frac{4[lipid][\alpha - syn]}{L}}}{2[\alpha - syn]} \tag{S4}$$

where K_D (in M) is the dissociation constant and L is the number of lipid molecules interacting with one molecule of α-synuclein.

4 Differential Scanning Calorimetry - data analysis

The enthalpy associated with the transition at 25°C was analyzed using the following assumptions. The protein:lipid ratios used in Fig. 1*B* are between 1:200 and 1:5. At these protein:lipid ratios and below 25°C, all the lipid molecules are in contact with monomeric protein molecules whereas the protein molecules, being in excess, are present both in solution and bound to DMPS. When the temperature reaches 25°C, there is a strong heat effect that includes contribution from several processes, including adsorption of additional protein (corresponding to differences between 1:350 and 1:30 P:L ratios), protein conformational changes and a phase transition of the membrane from the gel to the fluid phase. Each one of these enthalpy contributions is to a first approximation proportional to the number of lipid molecules involved, and the overall change in enthalpy measured at 25°C can therefore be described as follows:

$$\Delta H_{cal,25^\circ C} = x_{lipid_B}(\Delta H_{cal,m} + \Delta H_{cal,b} + \Delta H_{cal,f}) \tag{S5}$$

where $\Delta H_{cal,m}$, $\Delta H_{cal,b}$ and $\Delta H_{cal,f}$ are, respectively, the enthalpy of melting of the lipids, the binding of α-synuclein to the lipids and the folding of the protein into an α-helix, respectively, and x_{lipid_B} is the fraction of lipid molecules bound to the protein. Using the same binding model ($\alpha - \mathrm{syn} + \mathrm{lipid_L} \rightleftharpoons \alpha - \mathrm{syn(lipid)_L}$) as that used to analyze the CD data, the fraction of lipids bound to the protein in the PL complex for any given $[\alpha - syn] : [lipid]$ ratio was calculated using the following equation:

$$x_{lipid_B} = \frac{(K_D L + [\alpha - syn]L + [lipid]) - \sqrt{(K_D L + [\alpha - syn]L + [lipid])^2 - 4[lipid][\alpha - syn]L}}{2[lipid]} \tag{S6}$$

5 Estimation of the surface area per DMPS molecule in the fluid phase

Since the surface area per DMPS molecule (A_l) in the fluid phase was not available from the literature, we estimated this value using the following equations:

$$A_l = \frac{2V_l}{D_B} \tag{S7}$$

$$V_l = V_C + V_H \tag{S8}$$

where V_l, V_H, V_C are the molecular volume, the head group volume and the hydrocarbon chain of a lipid molecule, respectively, and D_B is the bilayer thickness[1, 2]. Using the value of V_C and D_B measured for DMPC molecules in the fluid phase, 782 Å^3 and 36.9 Å[1], respectively, and taking V_H for the PS head group, 244 Å^2 [1], we can estimate the A_l value of DMPS in the fluid phase to 55.6 Å^2.

6 Estimation of the energy of transfer of a lipid molecule from water to a bilayer

The free energy of transfer of a lipid molecule from water to a bilayer has been found to be approximately proportional to the number of aliphatic carbons in the lipid chain[2]:

$$\Delta G^\circ_{tr} = (\frac{\partial \Delta G^\circ_{tr}}{\partial n_{CH}}) n_{CH} + \Delta\Delta G^\circ_{tr,\circ} \tag{S9}$$

where $\frac{\partial \Delta G^\circ_{tr}}{\partial n_{CH}}$ and $\Delta\Delta G^\circ_{tr,\circ}$ are the gradient and intercept, respectively, of a linear plot. This linear dependence was shown to hold for lipids with zwitterionic (phosphatidyl choline (PC)) and negatively charged (phosphatidyl glycerol(PG)) head groups and chain lengths ranging from 8 to 18 aliphatic carbons[2]. We used the linear dependence of $\frac{\Delta G^\circ_{tr}}{RT}$ known for 1,2-dihexanoyl-sn-glycero-3-phospho-L-serine ($(6{:}0)_2$PS), 1,2-dioctanoyl-sn-glycero-3-phospho-L-serine ($(8{:}0)_2$PS) and 1,2-dilauroyl-sn-glycero-3-phospho-L-serine ($(10{:}0)_2$PS)[2–5], with $R = 8.314$ J.mol^{-1}.K^{-1} and $T = 303$ K to determine $\frac{\partial \Delta G^\circ_{tr}}{\partial n_{CH}}$ (PS) (-3.59 kJ.mol^{-1}) and $\Delta\Delta G^\circ_{tr,\circ}$ (PS) (2.49 kJ.mol^{-1}) for phosphatidyl serine (PS) ($R^2 = 1.0$). We then extrapolated this linear dependence to $n_{CH} > 10$, as observed for PC and PG lipids, and we estimated ΔG°_{tr} for DLPS ($(12{:}0)_2$, $n_{CH} = 12$), DMPS ($(14{:}0)_2$, $n_{CH} = 14$), DPPS ($(16{:}0)_2$, $n_{CH} = 16$), POPS ((16:0)/(18:1), $n_{CH} = 17$), DOPS ($(18{:}1)_2$, $n_{CH} = 18$) using Eq. S9, $\frac{\partial \Delta G^\circ_{tr}}{\partial n_{CH}}$ (PS) and $\Delta\Delta G^\circ_{tr,\circ}$ (PS).

SI Figures

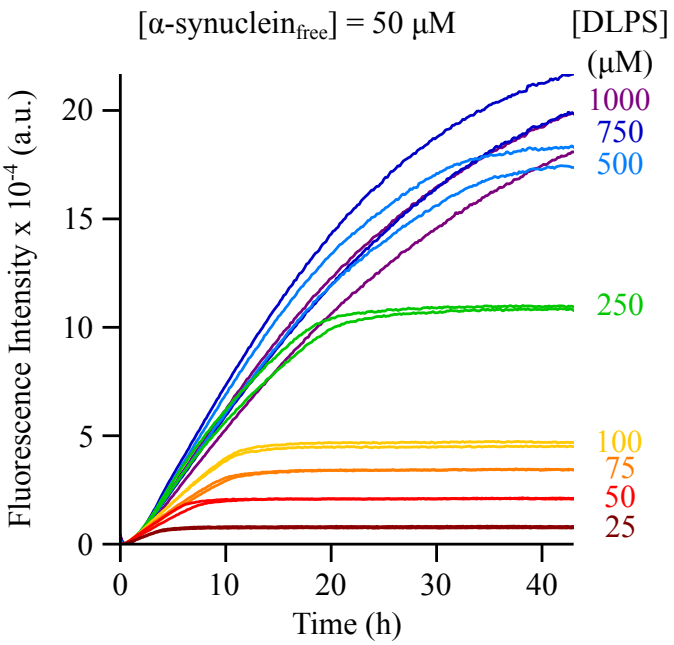

Fig. S 1: The concentration of fibrils formed by α-synuclein in the presence of DLPS is proportional to the concentration of lipid. Change in the fluorescence signal of the ThT when 50 μM α-synuclein is incubated in the presence of increasing concentration of DLPS (25 (dark red), 50 (red), 75 (orange), 100 (yellow), 250 (green), 500 (blue), 750 (dark blue) and 1000 (purple) μM).

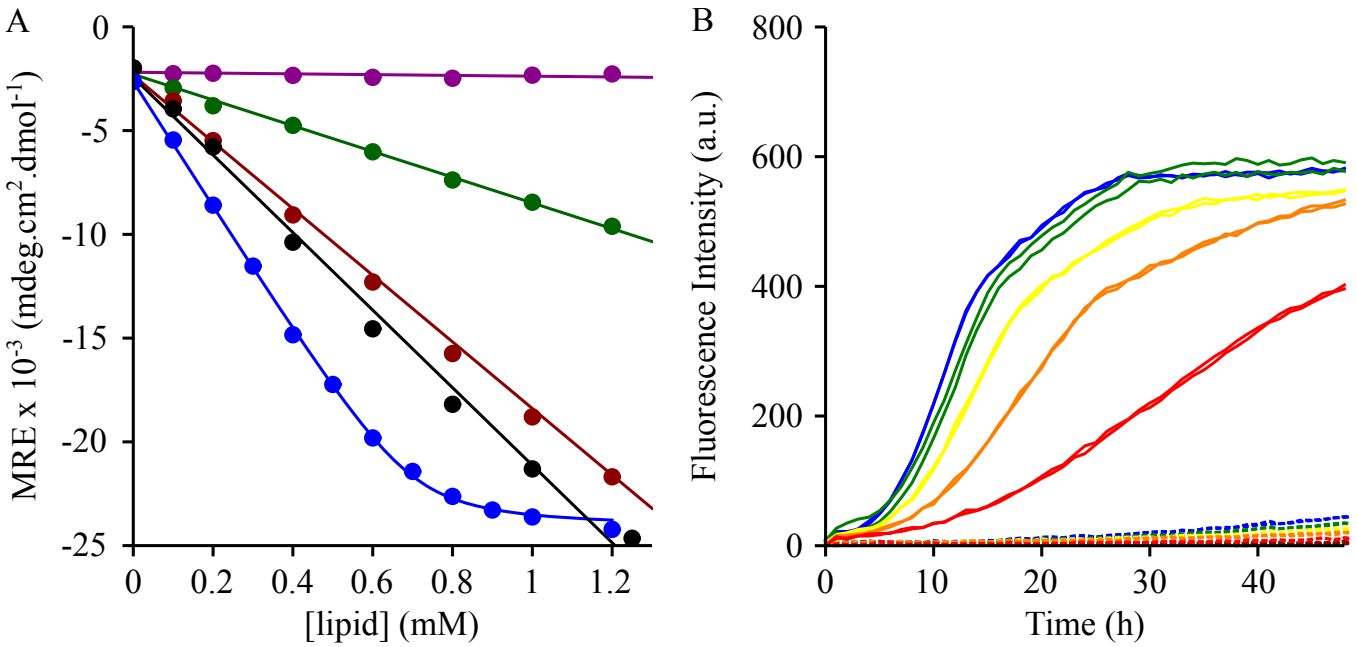

Fig. S 2: Effects of a change in the charge of the model membranes on the binding of α-synuclein and the kinetics of amyloid formation. (*A*) Change in the Mean Residual Ellipticity at 222 nm of α-synuclein (20 μM) incubated at 30°C in the presence of increasing concentrations of DMPC:DMPS (M:M) model membranes (DMPC:DMPS = 0:100 (blue), 25:75 (black), 50:50 (dark red). 75:25 (dark green), 100:0 (dark purple). (*B*). Evolution of the ThT fluorescence signal when 20 (red), 40 (orange), 60 (yellow), 80 (green) and 100 (blue) μM α-synuclein is incubated in the presence of 100 μM DMPS (solid line) or DMPC:DMPS (25:75) (dotted lines) and when 100 μM α-synuclein is incubated in the presence of 100 μM DMPC:DMPS (50:50, M:M) (dark red), DMPC:DMPS (75:25, M:M) (dark green) or DMPC (dark magenta).

References

[1] Petrache, H. I, Tristram-Nagle, S, Gawrisch, K, Harries, D, Parsegian, V. A, & Nagle, J. F. (2004) Structure and fluctuations of charged phosphatidylserine bilayers in the absence of salt. *Biophys J* **86**, 1574–1586.

[2] Marsh, D. (2013) *Handbook of Lipid Bilayers*. (CRC Press, Boca Raton, FL).

[3] Marsh, D. (2012) Thermodynamics of phospholipid self-assembly. *Biophys J* **102**, 1079–1087.

[4] Kleinschmidt, J. H & Tamm, L. K. (2002) Structural transitions in short-chain lipid assemblies studied by ^{31}P-NMR spectroscopy. *Biophys J* **83**, 994–1003.

[5] Walker, J. M, Homan, E. C, & Sando, J. J. (1990) Differential activation of protein kinase C isozymes by short chain phosphatidylserines and phosphatidylcholines. *J Biol Chem* **265**, 8016–8021.